Resonant Pumping of Er-Doped Fiber Amplifiers for Improved Laser Efficiency in Free-Space Optical Communications

Malcolm W. Wright,* Haomin Yao,† and John R. Marciante†

ABSTRACT. — An efficient laser transmitter design is proposed using resonant pumping of an erbium-doped fiber amplifier for a free-space optical communications source. Preliminary results are compared with fiber models to understand the influence of various design parameters in order to optimize the power conversion efficiency. An overall efficiency of greater than 20 percent should be realizable based on current designs with optimized pump sources.

I. Introduction

Fiber laser transmitters for free-space optical communications are based on the telecommunications industry investment in highly reliable and compact sources that have been developed at the 1.5 μm wavelength. This wavelength is the optimum for low-loss transmission through fiber, motivating extensive component development to support high data rates. Fortunately, the atmosphere is largely transparent in this wavelength range, so robust free-space links can be demonstrated with existing technology. Since the laser source is the dominant power draw in a spaceborne optical communications system, power efficiency is a key factor in the design of the laser transmitter. However, in contrast to space-based systems, overall efficiency is not a strong cost driver for terrestrial markets. The choice of laser is driven by the need for high data rates in a compact space-qualifiable package. Additionally, the ability to leverage the component development of terrestrial telecommunications and other industrial applications has led the design to be based on master-oscillator/fiber-power-amplifier configurations rather than the traditional solid-state laser systems. These fiber lasers have demonstrated power conversion efficiencies on the order of 20 percent using ytterbium- (Yb)-doped amplifiers at 1 μm [1]. However, to leverage the significant investment and reliability heritage of terrestrial telecommunication systems, there is a strong motivation to be based at the 1.5 μm lasing wavelength of erbium- (Er)-doped or Er/Yb-doped fiber amplifiers (EDFAs). The optical conversion efficiencies at this wavelength are

* Communications Architectures and Research Section.
† Institute of Optics, University of Rochester, Rochester, New York.

The research described in this publication was carried out by the Jet Propulsion Laboratory, California Institute of Technology, under a contract with the National Aeronautics and Space Administration.

currently more limited to less than 20 percent, typically 10 percent due to the use of highly reliable, high-power 980-nm, semiconductor pump laser diodes [2]. Even though these devices have shown large improvements in efficiency (over 60 percent electrical-to-optical efficiency has been demonstrated [3] under the Defense Advanced Research Projects Agency [DARPA] Super High-Efficiency Diode Sources [SHEDS] program), the quantum defect of the mismatch in pump-to-signal wavelength still ultimately limits the potential for higher efficiency in the amplifier, the main power draw in a fiber laser. To seek higher efficiencies, a new paradigm is required.

Recent diode development has addressed this with the availability of high-power pump diodes at 1480 and 1530 nm. Though their maturity and reliability has not yet been demonstrated to levels comparable to 980-nm diodes, these diodes offer the potential for significantly improving the power efficiency of fiber amplifiers, and hence fiber laser transmitters in general, while still enabling leverage of the investment in the remaining reliable components from the terrestrial telecommunications industry. Note that due to the unique requirements of free-space laser transmitters for deep space, which require high link efficiency and hence use the more energy-efficient pulse-position modulation (PPM) data formats with high peak powers, standard fiber telecommunication components may not be applicable [4]. The latter is mostly in the development of polarization-maintaining large-mode-area fibers to support the high peak powers and low radiation susceptibility.

This article highlights (a) the design of a fiber-based laser transmitter using resonant pumping of the optical amplifier, (b) comparison of the experimental results in a preliminary model from a vendor of commercially available fiber, and (c) comparison with a more detailed model developed at the University of Rochester. Preliminary experimental results will be presented that lead to an upgraded design that is still under development. The advantages of resonant pumping are clearly demonstrated, although the optimized design is far from realized in the current experiment. Section I gives an overview of the physics of resonant pumping and discusses the system efficiency, comparing to other published work in Section I.A. Section I.B introduces the commercial simulation tool used initially to design the fiber amplifier, and discusses the factors influencing the expected performance for various configurations. Section II outlines the experiment in II.A and preliminary results in II.B, with Section III discussing the University of Rochester fiber model. Finally, in Section IV we compare these designs to the current experiment, discuss its limitations, and highlight the path to optimization for an experimental demonstration of a high-efficiency Er-doped fiber amplifier.

II. Fiber Amplifier Design

A. Efficiency Estimates

The absorption spectrum of erbium allows for pumping at 980 nm, though the transfer and relaxation mechanism is more accessible when Yb ions are co-doped in the matrix with pumping at the same wavelengths, as shown in Figure 1. Yb^{3+} ions absorb the pump light and transfer energy to the excited state of Er for lasing on the Er^{3+} $^4I_{15/2} - {}^4I_{13/2}$ transition. Much larger dopant concentrations of Yb ions compared to Er ions are possible in the

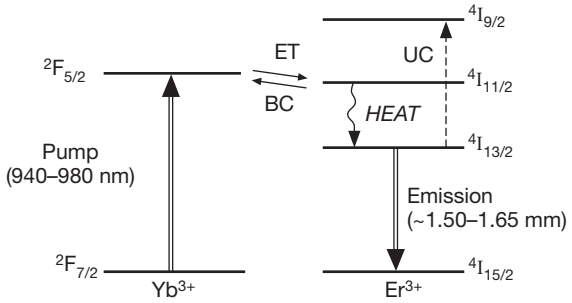

Figure 1. Energy transfer from Yb^{3+} to Er^{3+} where ET = energy transfer, BC = backconversion, and UC = upconversion [5].

glass fiber, which increases the pump absorption and is a key factor in high-power optical amplifiers. Unfortunately, the mismatch in pump and signal wavelengths, referred to as the quantum defect, enforces a limit on the optical-to-optical conversion efficiency. Moreover, parasitic lasing on the Yb system at 1 μm also limits the 1.5 μm output at very high pump powers. By pumping in the Er^{3+} system alone at 1530 nm from $^4I_{15/2} - {}^4I_{13/2}$ manifold, and lasing at >1550 nm, the overall optical efficiency is significantly enhanced, although it behaves as a quasi 3-level system. Even though relaxation is a potential loss mechanism and filling of the ground state limits the inversion since the lasing transition is in the absorption window, an increased optical-to-optical efficiency should be realizable.

The availability of high-performing reliable pump lasers at 1530 nm has been the main limit to achieving these higher efficiencies since the amplifier configuration is the main power loss process. Recent Department of Defense–sponsored work is addressing this with multiwatt devices becoming available in suitable fiber-coupled pump module packages. The electrical-to-optical (E-O) efficiency of these devices is limited due to Auger recombination processes in the quantum-well material at longer wavelength, so maximum E-O efficiencies of up to only 40 percent have been demonstrated in research devices [6]. The other factors in determining the amplifier efficiency are as follows:

$$\eta_{\text{amp}} = \eta_{\text{EO}} \eta_{\text{P}} \eta_{\text{O}}$$

where η_{EO} = pump diode electro-optic efficiency, η_{P} = pump launch and absorption efficiency, and η_{O} = optical-optical or slope efficiency and includes the quantum defect, η_Q. For comparison, the efficiencies for various pump configurations are shown in Table 1.

The optical-to-optical efficiency for 1530 nm pumped fiber in Table 1 is taken from data in Table 2 on what has been published recently for similar systems. Note that core pumping is not applicable to multiwatt amplifiers as required for deep-space optical communications; hence, a dual-clad geometry is required. In a dual-clad fiber, the pump light is injected into the cladding surrounding the smaller core of the amplifier. As the pump light propagates down the fiber, it eventually crosses the core and is absorbed.

Table 1. Efficiency contributions for Er-doped fiber amplifiers at various pump wavelengths. The quantum defect for pumping at 976, 1480, and 1532 nm is 0.63, 0.94, and 0.96, respectively.

Efficiency	Yb-Er (976 nm)	Er (1480 nm)	Er (1532 nm)
Diode electrical-optical	0.5	0.35	0.4
Pump absorption	0.85	0.85	0.85
Optical-optical	0.43	0.7	0.7
Total	0.18	0.21	0.24

Table 2. Comparison of published optical-to-optical efficiencies in Er- and Er/Yb-doped fiber systems using core-pumped and dual-clad (DC) geometries. Slope efficiencies include all launched pump power; absorbed values exclude unabsorbed pump light emitted from the fiber.

Pumping Geometry	Dopant	Fiber Geometry	Power, W	Pump λ, nm	Signal λ, nm	Opt-Opt Efficiency, %	Opt-Opt Measurement	Ref.
Core	Er	MOPA	0.2	1480	1570	60	Slope	[7]
Core	Er	MOPA	0.3	1480	1560	84	Slope, launched	[8]
DC	Er	MOPA	3.5	980	1570	22	Slope	[7]
DC	Yb/Er	Laser	100	980	1532–1568	43*	Slope, launched	[9]
DC	Yb	Laser	<1 (>>1 more recent)	980	~1100	90†	Slope (absorbed, 85% meas. slope, 70% wrt launch)	[11]
DC	Er	Laser	48	1530	1590	57	Slope, narrow Δλ pump	[10]
DC	Er	MOPA	9	1530	1570	46	Absorbed (33% slope)	[12]
DC	Er	MOPA	67	980	1570	30	Absorbed (est.) slope	[13]
DC	Er	Laser	88	1530	1590	69‡	Slope (absorbed pump)	[14]

* Maximum efficiency of 1.5-μm laser pumped at 980 nm
† Maximum efficiency of 1-μm laser
‡ Maximum efficiency of 1.5-μm pumped in dual-clad geometry with 1530 nm

B. Preliminary Fiber Model

The first fiber model was based on the Liekki Application Designer (LAD) design tool from nLIGHT [15]. A single-stage master oscillator power amplifier (MOPA) configuration was set up with dual-clad (DC) pumps for continuous wave (cw) operation, as shown in Figure 2.

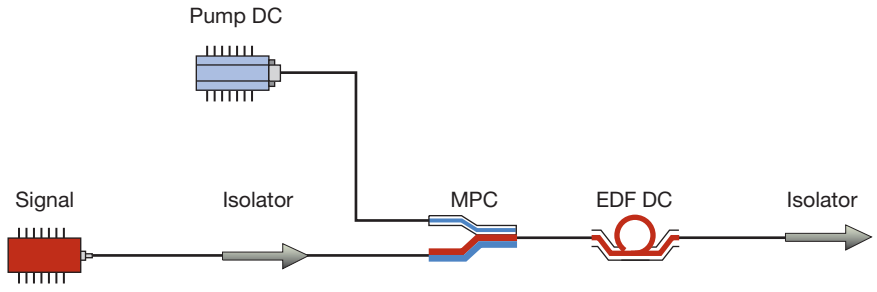

Figure 2. LAD fiber model. MPC is a multimode fiber pump combiner, and EDF is the Er-doped fiber amplifier in a dual-clad configuration.

Parameter values were based on the actual Liekki fiber used in the experiment, Er60-20/125. A 10-W pump centered at 1530 nm (no linewidth broadening) was used to compare with our experiment. The fiber absorption and emission cross sections shown in Figure 3(a) were used with a 12-m length of active fiber. The net small-signal (unsaturated) gain, G, is plotted in Figure 3(b) for various inversion levels according to

$$G(\lambda) = \left(\sigma_{\text{emiss},\lambda} N - \sigma_{\text{abs},\lambda}(1-N)\right).L$$

Where σ_{emiss}, σ_{abs} are the emission and absorption cross section, respectively; N is the fractional population inversion; and L is the length of the fiber.

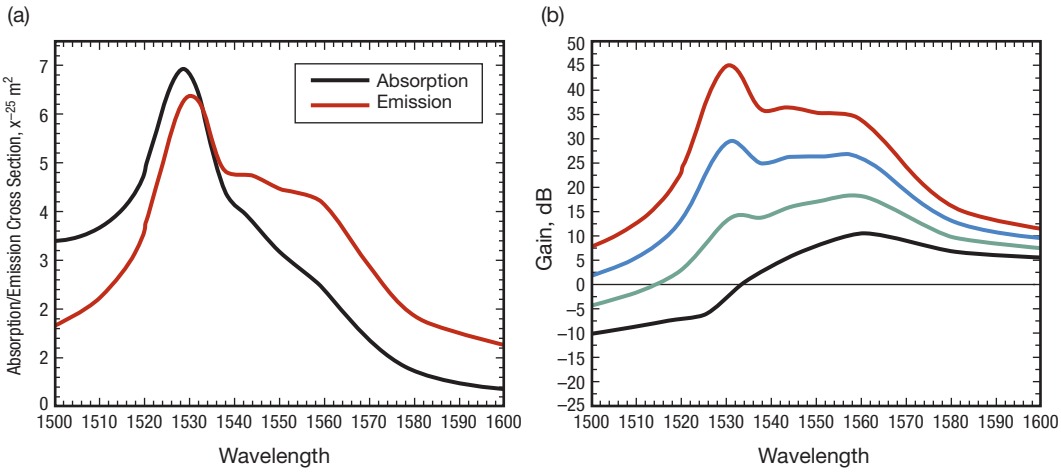

Figure 3. (a) Fiber absorption and emission cross sections, and (b) net small-signal gain for various inversion levels increasing from 50, 60, 70, and 80 percent with increasing gain and 12-m length.

The output of the model is shown in Figure 4 for various pump and signal wavelengths. Also shown in Figure 4(b) is the pump power along the length of the fiber.

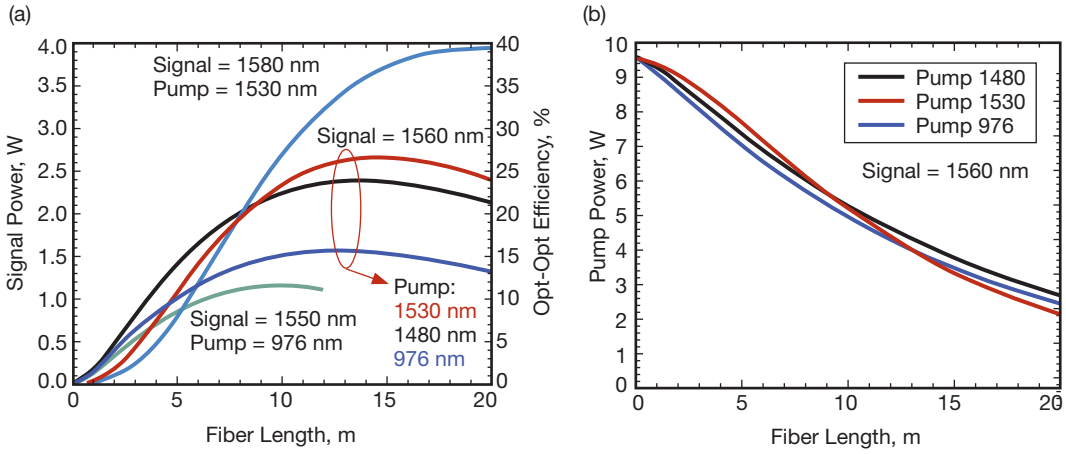

Figure 4. (a) Signal and (b) pump power along the fiber length for various signal and pump wavelengths.

As can be seen from Figure 4(a), 976-nm pumps represent the most inefficient power conversion with a small increase in going to longer signal wavelengths. Pumping with 1480 nm improves the power conversion; however, the most efficient power conversion is seen with 1530-nm pumps and signal wavelength of 1580 nm. Pump power is not greatly affected by the choice of pump wavelength, suggesting the presence of excited-state absorption or upconversion processes, which will be explored in the latter model.

To understand in more detail the issues affecting the power conversion efficiencies rolled up in the overall power numbers shown in Figure 4, it is helpful to look at the intrinsic properties of the fiber in these various configurations and understand where the losses might be occurring. Since the signal gain is driven by the inversion level and degraded by amplified spontaneous emission (ASE), these values were calculated from the model both along the fiber length and as a function of wavelength for a range of input signal and pump wavelengths. Representative output results are shown in Figure 5 (next page) for typical seed laser powers of 20 mW and pump powers of 10 W unless otherwise noted.

Some immediate observations are possible, noting that increased ASE in the fiber robs the gain from the signal or seed wavelength: the shorter the pump wavelength, the higher the initial inversion but less ASE output; the longer pump wavelength has more uniform inversion and higher output ASE, but increasing the seed wavelength lowers that significantly. Though more power is output for longer seed wavelengths, more ASE is in the fiber for longer wavelengths, which suggests that improvement in power could be obtained if this can be reduced by, for example, spectral filtering or using multistage amplifiers. The increased ASE along the forward direction suggests that pumping in a backward propagating configuration should enable lower ASE and hence increased signal power in the output. Experimentally, this is somewhat challenging with the currently available devices and pump combiners. In summary, Table 3 highlights some design considerations.

Table 3. Fiber amplifier design criteria for pump and signal wavelength dependence.

Choose Seed Wavelength to:	Parameter
Minimize ASE output	Longer seed λ
Increase inversion	Small seed λ dependence
Maximize signal power	Longer pump λ
Minimize unabsorbed pump power	Longer seed λ

Another design aspect is highlighted by considering the input signal power dependence in Figure 6. Increasing the signal power improves the power conversion efficiency significantly, as evidenced by a corresponding reduction in ASE (not shown).

The fiber model also includes a cluster concentration parameter to account for clustering of the Er ions, which acts as a loss mechanism for excited-state population generation. Though the exact level of clustering is difficult to measure, the output power is strongly dependent on large variations. Decreasing the concentration from the nominal model value of 3.6 percent to 2 percent increases the signal output power from 2.5 W to 3.5 W in the model with 1530-nm pumping and 1560-nm signal wavelength.

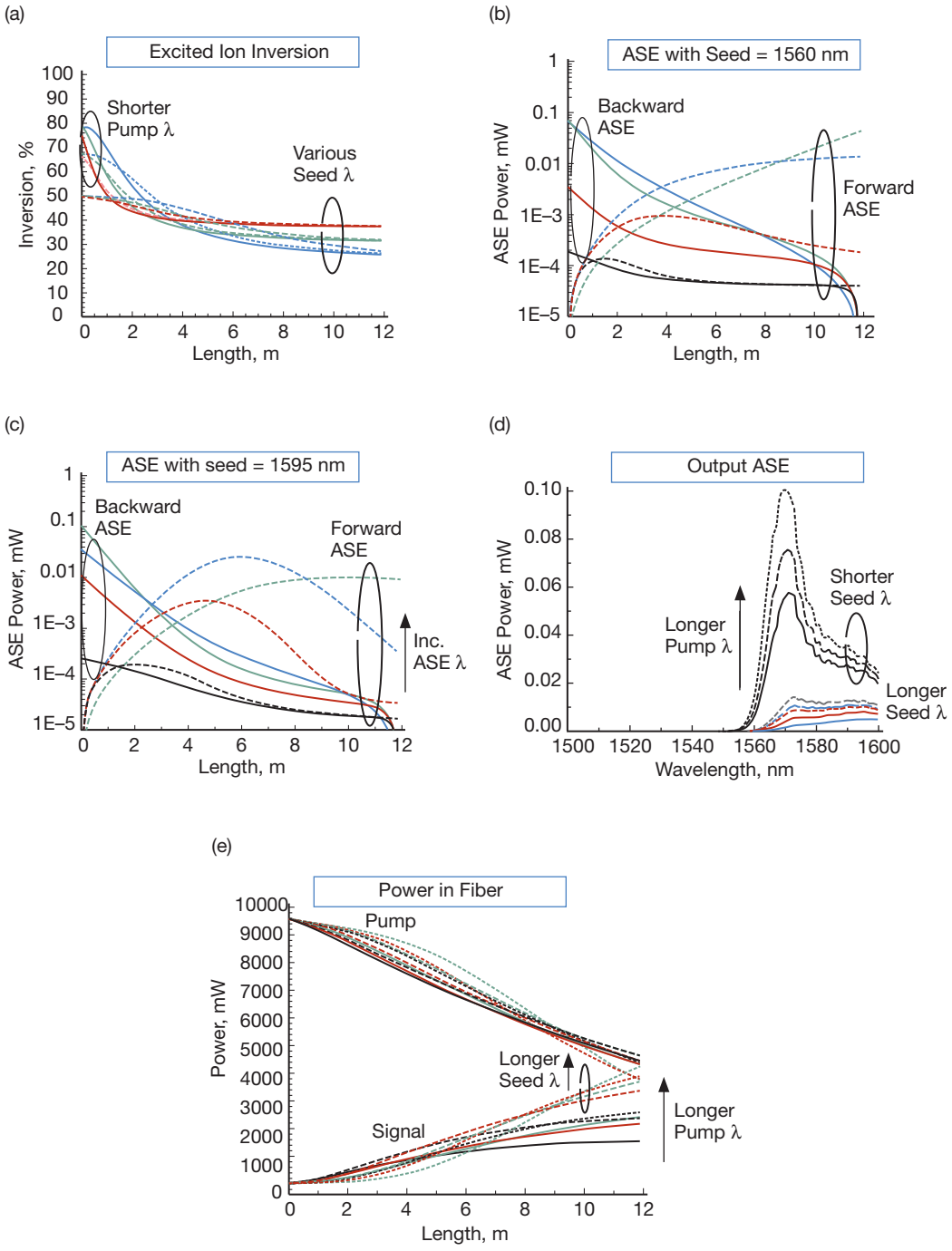

Figure 5. (a) Population inversion level along fiber for signal wavelengths of 1560 nm (red), 1575 nm (green), and 1595 nm (blue), and pump wavelengths of 980 nm (solid), 1480 nm (dotted), and 1530 nm (dashed); (b) forward (dashed) and backward (solid) propagating ASE at 1530 nm (blue), 1550 nm (red), 1560 nm (green), and 1580 nm (blue) for a seed wavelength of 1560 nm and a pump wavelength of 1530 nm; (c) same as (b) for 1595-nm seed wavelength; (d) output ASE spectra for pump wavelengths 980 nm (solid), 1480 nm (dashed), and 1530 nm (dotted) and seed wavelengths of 1560 nm (black), 1575 nm (red), and 1595 nm (blue); (e) Power in the fiber for the same conditions as (d) with 1595 nm as green instead of blue.

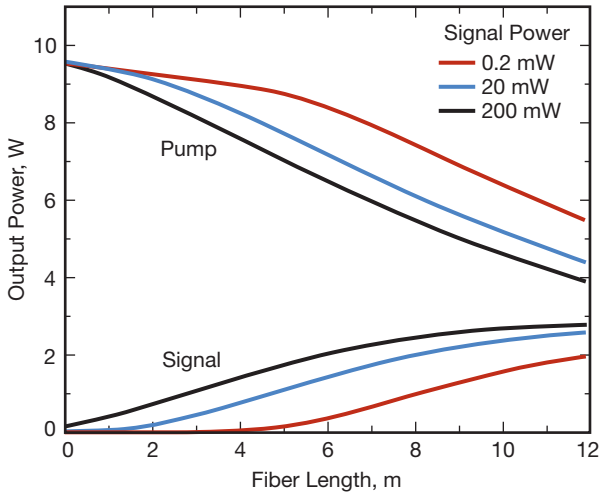

Figure 6. Power along fiber for 1530-nm pump and 1560-nm signal wavelength with 0.2 mW (red), 20 mW (blue), and 200 mW (black) signal input powers.

II. Fiber Amplifier Experiment

A. Experiment Setup

Fiber-coupled pump diodes were procured from several vendors. Although single-element devices provide the best path to efficiency as is used for standard 980-nm EDFA pumping, many such devices are required to produce the 10 W of pump power needed for our configuration. Although preliminary devices involved multiple elements in some of the packages to reach these powers, recent development shows that single-element, narrow-linewidth modules are becoming available on a custom basis [6]. Nominal 4-W cw power out of the fiber was available in either a broad spectral output or in a narrow linewidth device. Ideally, a spectrally narrowed source is desired, but the efficiency of such commercial devices is still quite low even compared to broad-area devices, with typically electro-optic efficiency in the range of 10 to 20 percent. Data for two of three devices are shown in Figure 7, with the third similar to the first device. Temperature tuning is required to match the emission with the fiber absorption, and it is apparent that both of these devices are able to cover the target erbium absorption peak around 1530 nm. In the fiber host, the erbium absorption peak is slightly shifted to near 1532 nm.

The output of these diodes was delivered in a 100/125 μm (core/clad) fiber that was then fusion spliced to a fiber combiner from Liekki. This (1+6):1 port device allowed up to six pump diodes to pump the dual-clad fiber amplifier in a MOPA design with co-propagating geometry for the pump and signal beams. The amplifier fiber was Liekki Er60-20/125 from nLIGHT. This fiber was highly erbium-doped, yielding a pump absorption rate of 60 dB/m in the 20-μm core. The cladding was a 125-μm dual-clad design with octagonal cladding for mode mixing of the pump light. This fiber was chosen because of its dual-clad design that allowed pumping with multimode diodes, its suitability for long-wavelength pumping, and its commercial availability. Previous experiments had also used similar fiber [7]. A mode field adaptor (MFA) was required to interface the single-mode seed diodes with the 20-μm core of the signal leg of the fiber combiner. The seed diodes were operated cw with 20 to

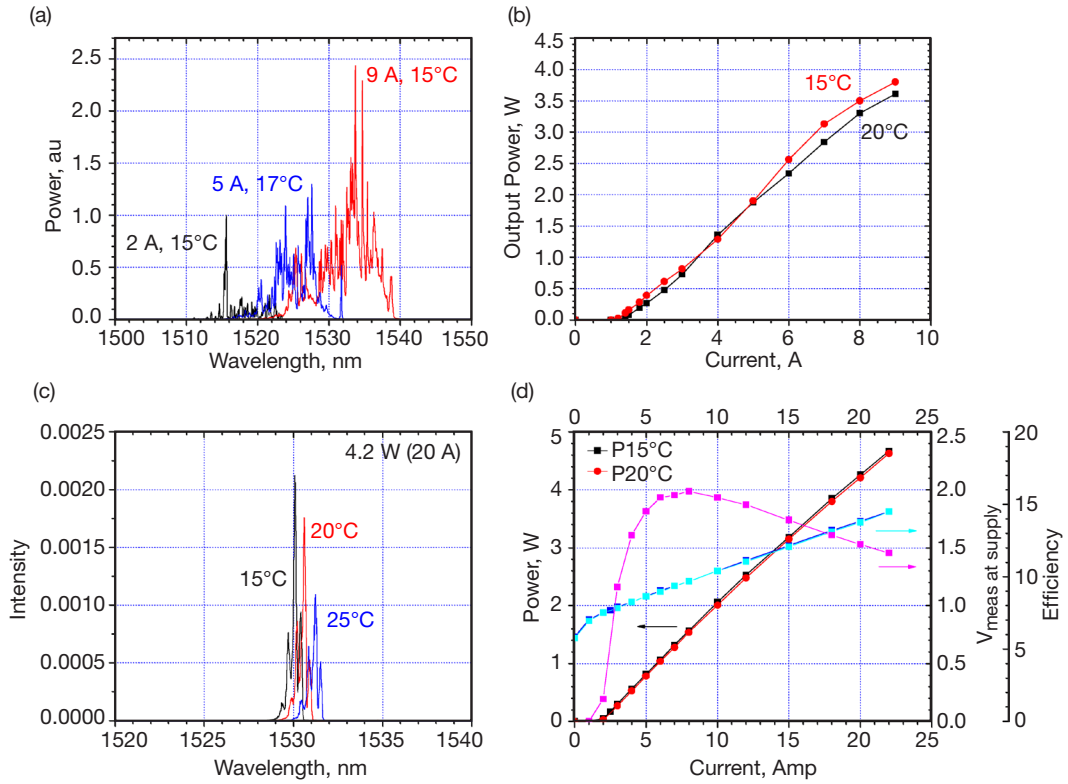

Figure 7. Pump diode results: (a) power, and (b) spectra for PLI device; and (c) power, and (d) spectra for QPC Lasers device. E-O efficiency of PLI unit is on the order of 10 percent at high power.

60 mW possible from 1564 to 1595 nm. The fiber amplifier output was angle-cleaved to limit optical feedback at the ends of the amplifier, and the seed laser was optically isolated as well. All components were fusion spliced for high-power operation, except for the input signal, which was connectorized. The splice losses were estimated to be ~0.1 dB when the fiber numerical apertures (NAs) were matched, and 0.2 dB when there was slight mismatch (0.15 to 0.22 NA) based on previous experience.

B. Results and Discussion

The fiber amplifier output is shown in Figure 8 when all three diodes are operated and temperature-tuned to maximize the signal output observed both on an optical spectrum analyzer and through a 3-nm narrow-bandpass filter centered on the laser line.

The emitted signal power was up to 1 W, corresponding to pump leakage or unabsorbed pump on the order of 3 W in the range 1520 to 1540 nm. The contribution from the ASE pedestal around 1565 nm was negligible (>35 dB lower than the signal) with a seed wavelength of 1560 nm. These values correspond to less than 50 percent of what was predicted with our preliminary model. The main difference is in the broad linewidth of two of the pump sources so that not all pump light is absorbed by the erbium ions. Other factors include the presence of excited-state absorption (ESA), upconversion, and pair-induced quenching, which will be introduced briefly here and described in more detail in the next

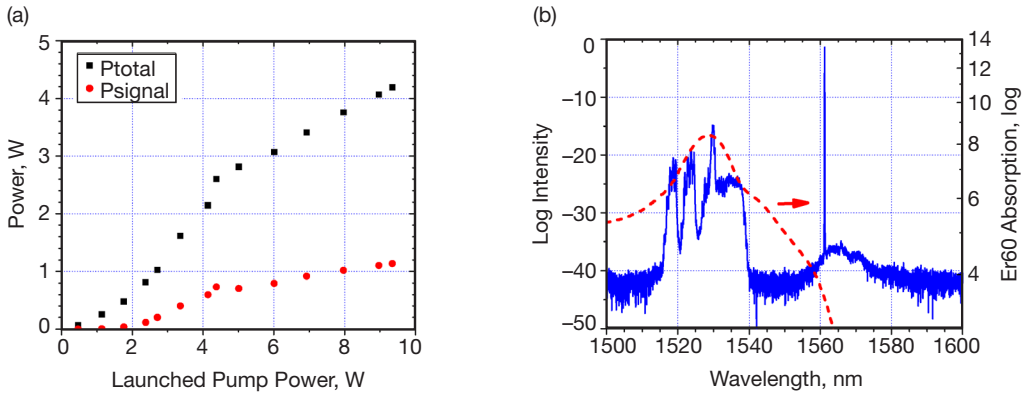

Figure 8. Amplifier output (a) power and (b) spectra as the pump current is increased. The Er absorption line is overlapped for reference.

section. Doping erbium ions into the glass matrix with high doping density is problematic, as it is for any rare earth ion. When the doping density is sufficiently high, two erbium ions can form a pair, of which only one can absorb pump light and be excited into the state; the other ion of the pair must remain in the lower state. This process is called pair-induced quenching. ESA is a process in which an erbium ion that has just absorbed a pump photon absorbs a second pump photon, elevating the excited-state electron into a state that rapidly loses its energy to the host medium via phonon-induced interactions. ESA is not explicitly included in the basic fiber model [15] and points to the need for a more detailed fiber model, which will be addressed in the next section. ESA is not expected to be dominant around 1530-nm pumping [5], but quenching of the upper state lifetime is known to be important, especially for highly doped fibers, such as is the case for our amplifier. Upconversion is a process in which an erbium ion in the excited state gives this energy to a neighboring erbium ion that is also in the excited state. The transferred energy kicks the electron into yet higher (unstable) energy levels, and the energy is once again lost to the host medium via phonon-induced interactions. Upconversion processes are dominant for the large doping densities, which are required to yield reasonable absorption lengths for dual-clad fibers. Longer seed wavelengths were also investigated, but the increased power efficiency was not apparent, only increased ASE emission. The maximum signal power at 1595 nm was ~0.8 W, with total ASE ~0.6 W. Higher input signal powers may be needed to operate the amplifier in a more saturated regime at the longer wavelengths where the net gain is lower, although the modeling shown in Figure 6 suggests that this should be only a slight difference. Intermittent lasing on the gain peak also occurred around 1565 nm. These results point to the need for a more detailed model that includes these additional effects to (a) simulate more accurately the observed experimental results, (b) and provide a more reliable path to efficient amplifier design.

III. Fiber Amplifier Model

A. Model Development

Given the ultimate target data rates (200 kHz to 100 MHz), an average-power model is appropriate to capture average power and inversion characteristics [4]. Modeling high-effi-

ciency, high-power EDFAs while accounting for all pertinent physical phenomena requires a model that

- is axially resolved (i.e., a propagation model for multimode dual-clad and single-mode core),
- is spectrally resolved,
- includes counter-propagation,
- captures upconversion and clustering effects, and
- accounts for large-mode-area (LMA) dual-clad fibers.

Our initial model [16] took into account all of these factors apart from excited-state absorption, upconversion, and clustering effects. These three factors, while essentially nonexistent in modern ytterbium-doped fiber amplifiers, play an important role in high-power erbium-doped fiber amplifiers, as noted above. Although pair-induced quenching due to clustering is usually intentionally avoided in ytterbium-doped fibers, the effect cannot so easily be avoided in erbium-doped fibers, which would otherwise be limited to 10× lower doping density. The effect on amplifier design is that although the doping density, in principle, can be increased, the effective doping density does not increase linearly.

The second factor is ESA. Due to the location of the Stark-split bands of erbium in the glass matrix, some excited states in the upper manifold can be excited to even higher states in an even higher manifold by the same pump wavelength. However, this state is not metastable, so the hyper-excited electron rapidly decays nonradiatively to the conventional metastable excited state. The net result of this action is that although two pump photons were required to put both ions into an initial excited state, only one ion ends up in the excited state and is available for extraction of optical gain. The net effect is a reduction of amplifier efficiency since pump energy is effectively lost nonradiatively to the glass medium. Unlike clustering, which is dependent on the total doping density, ESA is only dependent on the fraction of the density that is inverted, that is, in the excited state.

The third factor is upconversion. If an excited ion is in sufficiently close proximity to another excited ion, an energy transfer can occur between the two ions. In this reaction, one excited ion loses its energy to the other and ends up in the ground state. The ion that receives the energy is excited to an even higher state. As with ESA, this state is not metastable, so the hyper-excited electron rapidly decays nonradiatively to the conventional metastable excited state, leaving a single excited state available for gain extraction at the expense of two pump photons. Like ESA, the net effect is a reduction of amplifier efficiency, since pump energy is effectively lost nonradiatively to the glass medium, and the process is only dependent on the fraction of the density that is inverted rather than the total population density. Nominally, all three of these effects are dependent on the particular composition of the glass matrix and can be affected by various other (not optically active) dopants.

All three high-doping-density effects were included into the model for accurate simulation of highly doped dual-clad EDFAs. A two-band system is modeled, which is exact for 1530-nm pumping (neglecting intraband dynamics), and a very good (commonly accepted)

approximation for 980-nm pumping since the excited pump state relaxes very rapidly to the metastable excited state of the lasing transition. The resulting propagation equation is given by

$$\mp\frac{dP_\lambda^\pm}{dz} = \Gamma_\lambda\left(\sigma_\lambda^e N_2^s - \sigma_\lambda^a N_1^s\right)P_\lambda^\pm + \Gamma_\lambda\left(\sigma_\lambda^e N_2^p - 2\sigma_\lambda^a N_1^p - \sigma_\lambda^a N_2^p\right)P_\lambda^\pm + \Gamma_\lambda\,\sigma_\lambda^e\left(N_2^s + N_2^p\right)h\nu_\lambda\,\Delta\nu - \alpha_\lambda^S P_\lambda^\pm + S\alpha_\lambda^R P_\lambda^\mp \quad (1)$$

where P is the power in wavelength bin l propagating in the ± direction, and N is the population in state 1 (ground) or 2 (excited) for single (s) or cluster-paired (p) bins; Γ_λ is the wavelength-dependent spatial overlap factor between the optical field and the erbium ions, σ_λ is the wavelength-dependent emission (e) or absorption (a) cross section, and $\Delta\nu$ is the spectral width of the wavelength bins. The wavelength-dependent scattering terms represent scattering loss (α^S) and Rayleigh scattering ($S\alpha^R$).

Equation (1) defines the power propagation along the length of the fiber for light of any wavelength propagating in forward or backward directions. The first two terms on the right-hand side of the equation denote stimulated emission and absorption from the single ions and the ions paired due to clustering, respectively. The third term represents spontaneous emission, while the final two terms represent scattering loss and backward Rayleigh scattering, respectively.

The populations of the ground and excited states for the single and paired ions are given by

$$\frac{dN_2^s}{dt} = \sum_\lambda \frac{\Gamma_\lambda P_\lambda}{A_{Er} h\nu_\lambda}\left(\sigma_\lambda^a N_1^s - \sigma_\lambda^e N_2^s\right) - \frac{N_2^s}{\tau_2} - C\left(N_2^s\right)^2 \quad (2)$$

$$\frac{dN_2^p}{dt} = \sum_\lambda \frac{\Gamma_\lambda P_\lambda}{A_{Er} h\nu_\lambda}\left(2\sigma_\lambda^a N_1^p - \sigma_\lambda^e N_2^p\right) - \frac{N_2^p}{\tau_2} \quad (3)$$

where A_{Er} is the doped area of the erbium ions, τ_2 is the lifetime of the metastable state, and C is the ESA (upconversion) factor. The relationship between the populations is given by $N_1^s + N_2^s = (1 - 2k)N_T$ and $N_1^p + N_2^p = kN_T$, where N_T is the total erbium ion density. These equations are nominally solved in the steady state (dN/dt = 0). The first term on the right-hand side represents absorption and stimulated emission, respectively. The second term represents nonradiative recombination, while the final term in Equation (2) represents ESA.

B. Model Benchmarking

Benchmarking the model against other simulation and experimental results is necessary to provide a basis for realizing an optimized amplifier design in the current configuration. Simulation results from Becker's work [17] gave excellent agreement with the current model for predicting the gain in EDFAs. The second set of benchmarking was performed against experimentally demonstrated high-efficiency and high-power EDFAs, using as much data as can be gleaned from the experiments and only small realistic changes to assumed parameters. By comparing to published results with 1530-nm pumping, this set allowed for the

prediction of physically realizable amplifiers, giving confidence in the model's ability to design high-efficiency EDFAs.

Dubinskii's experiments were initially targeted since they have reported the highest EDFA efficiencies for various pumping and fiber configurations. The first experiment, and the highest reported efficiency to date (84 percent), was for an EDFA that was core pumped with 1476-nm pumps [8]. Figure 9 shows perfect agreement between our model and these experiments.

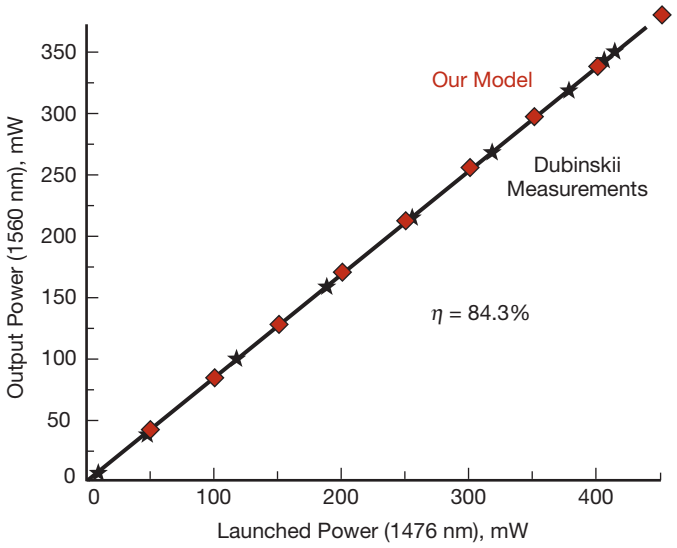

Figure 9. Output power at 1560 nm vs. launched pump power at 1476 nm: Dubinskii's experimental measurements (black) and our model (red).

The final configuration tested was for dual-clad fibers pumped at 1530 nm [12]. In this case, the experimental pump bandwidth was stated to be 20 nm. To account for this in our model, we modified the pump absorption and emission cross sections by averaging over the wavelength band of interest. This resulted in net lower absorption and net higher emission of the pump wavelength, reducing the predicted amplifier efficiency. Nevertheless, when accounting for this additional physics, Figure 10 shows excellent agreement between Dubinskii's experimental measurements and our model predictions.

It is important to point out the seeming disparities between Figures 9 and 10. Although both have small quantum defects, the efficiency disparity is large; 1476-nm pumping seems to offer 84 percent efficiency while 1530-nm pumping offers only 47 percent. However, this comparison cannot be made directly. The 1476-nm pumping case was core pumped, while the 1530-nm pumping case was cladding pumped. These cases offer substantially different operating regimes. For cladding pumping, the erbium doping density needs to be very high in order to compensate for the low overlap between the cladding-confined pump light and the core-confined erbium. Such a situation would otherwise result in a net reduction of pump absorption by a factor of A_{clad}/A_{core}, or about a factor of 40. This required high doping level, while imposing limitations due to ESA, is critical in simultaneously allowing both the required higher-power outputs and reasonable lengths of erbium-doped fiber.

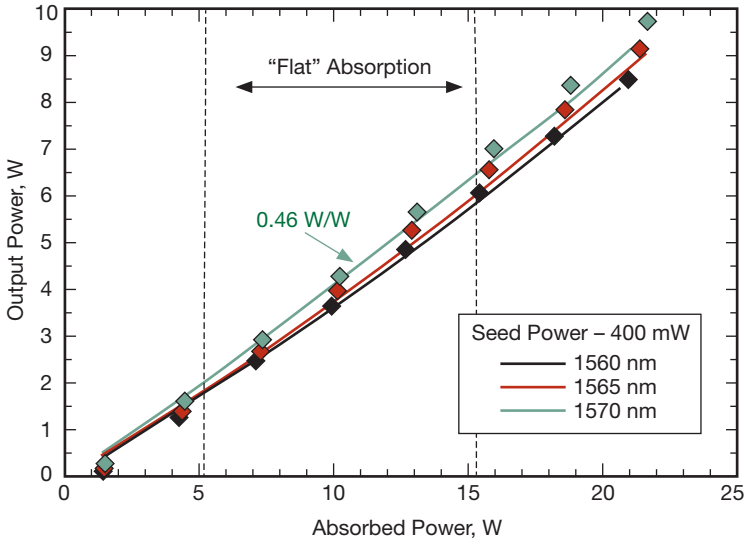

Figure 10. Output power vs. absorbed pump power at 1530 nm for various seed wavelengths: Dubinskii's experimental measurements (lines) and our model (diamonds).

A more subtle effect is the impact of the inversion level. Core pumping often leads to a nearly fully inverted population level, allowing for maximum signal gain and power extraction. Cladding pumping cannot typically achieve such high pump intensities, and therefore operates at lower inversion levels and therefore less power extraction. The subtlety comes in the fact that the amount of pump power required to sustain the lower doping-density core-pumped case is much less (~40×) than that required for the higher doping-density cladding-pumped case.

In all of the experimental comparisons presented in Figures 9 and 10, it was necessary to make some slight parameter adjustments to obtain these nearly perfect fits. In some cases, it was as simple as including isolator and coupler loss between the seed source and the amplifier. In others, it was necessary to tweak the cross sections by 5 to 10 percent. However, uncertainties in experimental parameters and measurements, as well as in some of the numbers used in the simulations, make such adjustments not only reasonable, but necessary. Further discussion on the impact of parameter variations will be given Section IV.

Based on the comparisons to established modeling results and published experimental results (Figures 9 and 10), it is clear that our model can accurately predict EDFAs at any pump and signal wavelengths, any pump configuration, and any fiber type. As such, our model is suitable for designing the high-efficiency, high-power EDFAs required for laser transmitters for free-space optical communications.

C. Model Results and Comparison with Experiment

Comparison with our preliminary experimental results was performed by using the Liekki Er60-20/125 fiber. Other parameters that were used in the simulation were either used from the experiment (12-m fiber length, 9.3-W pump power at 1530 nm, and signal wavelength of 1565 nm with 10 mW launched into the fiber core), taken from Liekki's fiber datasheet (area and NA for core and cladding, lifetime, clustering, scattering loss), calculated/extracted

based on experimental parameters (core mode confinement, cladding absorption overlap, doping density), or taken from the literature (Rayleigh backscattering, ESA). It is important to point out that most of these fiber parameters have reasonable error. For example, the core diameter is stated as 20 ±2 μm. This leads to a cladding absorption overlap (Γ_{pump}) that has ±20 percent uncertainty, which can severely affect the pump absorption. Moreover, parameters such as pair-induced quenching, ESA, and upconversion are not well known since most experiments are designed to avoid the region where these become important.

The detailed calculation results are shown in Figure 11. These plots show the signal, pump, and ASE evolution in the fiber, the inversion along the length of the fiber, and the output spectrum (plotted for a standard 0.1-nm resolution).

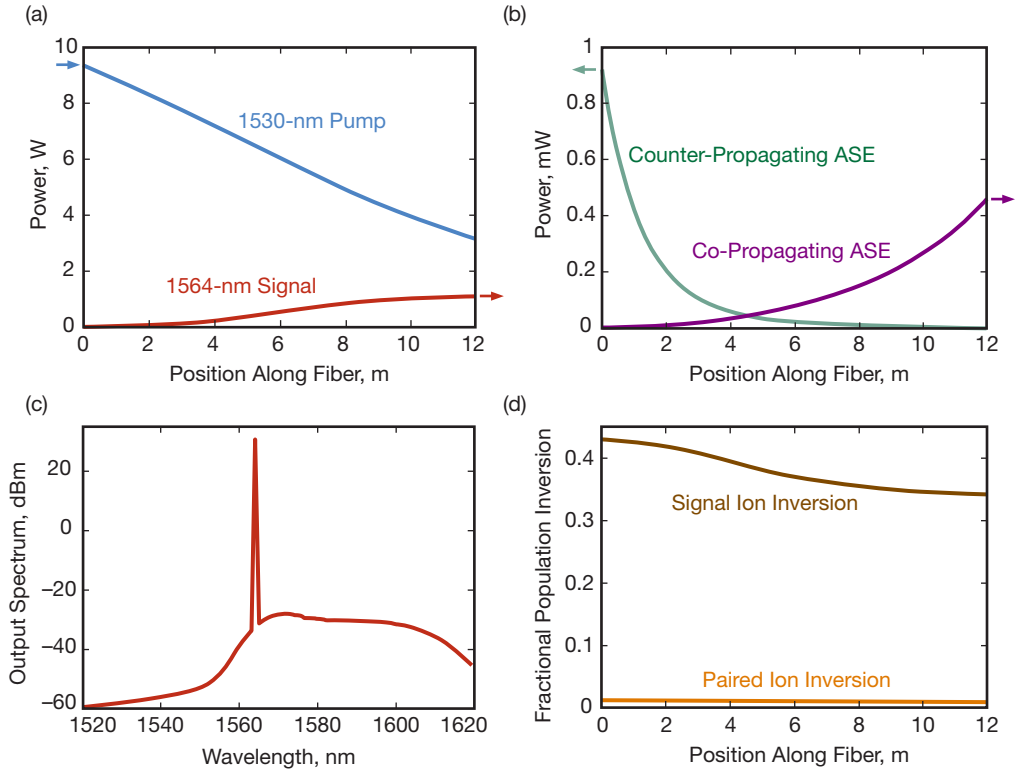

Figure 11. Simulations corresponding to experiments. (a) pump (blue) and signal (red) evolution in the amplifier; (b) co-propagating (purple) and counter-propagating (green) spectrally integrated ASE power; (c) output spectrum with pump removed; (d) population inversions of single (brown) and cluster-paired (gold) erbium ions.

Based on the pump absorption, it is reasonable to draw the conclusion that the fiber length should be longer to absorb the remaining pump. Doping concentration could also be increased, but this has the adverse effect of increasing defect concentration. However, the absorption cross section in Figure 3 suggests that the material is in fact not transparent, but rather absorbing in its nominal (unpumped) state. As such, a certain pump power level must be maintained in the fiber simply to allow it to remain transparent. This is also evident from the signal evolution, which seems to have reached a plateau at the end of the 12-m length of fiber, implying that a longer fiber would result in lower power output.

A summary of the results of the simulations as compared to the experiment are shown in Table 4 and show good agreement.

Table 4. Comparison between experimental and modeling results.

Parameter	Experimental Data	Simulated Result
Output Signal Power	1.1 W	1.1 W
Unabsorbed Pump Power	3.1 W	3.1 W

The good agreement is encouraging since, in spite of the reasonably large uncertainty in some of the parameters, the values for these simulations were kept in the middle of their respective ranges. The only exception was that the upconversion coefficient used was 15 percent larger than that used in the literature, a value that is not known to high precision.

IV. Path to Optimization

Given that 1530-nm pumping demonstrates the potential for high-efficiency operation, and validation of the model, the amplifier design is optimized to find the operating wavelength that provides the highest output power. In this optimization, the fiber length and pump configuration were allowed to vary in search of the optimal operating conditions. The total pump power (10 W) was kept constant, but the distribution between co-propagating and counter-propagating pump power was allowed to vary. For all cases, counter-pumping led to the highest signal output power. Two cases were studied in this optimization. The first represents the current experiments above with an input signal power of 10 mW. The second corresponds to more optimal conditions of 100 mW signal seeding. By reducing the amount of gain that needs to be provided by the final stage (multiwatt) amplifier, higher efficiency can be obtained.

The results of these studies are shown in Figure 12. For 100-mW seeding, counter-pumping yields the highest output power and highest efficiency, approaching 45 percent. For illustration, the co-pumping case is also shown. In this case, the amplifier suffers a significant efficiency hit, attaining a maximum of only 3.3 W. Although some engineering difficulties present themselves with counter-pumping, the advantages of this configuration are clear. Also shown in Figure 12 are the optimization curves for co- and counter-pumping for 10-mW seed. Interestingly, the counter-pumped case for the 10-mW seed provides nearly the same results as co-pumping with the 100-mW seed, implying that the gain is simply not being optimally extracted. Finally, the co-pumped case for 10-mW seeding shows even further reduction, similar to the reduction observed for the 100-mW seeding case. Interestingly, similar values are predicted (green curve) for the wavelength used in our experiments above, even though the fiber length is different in this configuration. Even at the optimal wavelength, the current experiment is predicted to yield a maximum of 23 percent. In contrast, by simply changing the pump geometry and seed power, almost twice the efficiency can be achieved.

It should be noted that these simulations were performed with all of the nominal values used previously except that the modified upconversion parameter used to match the experi-

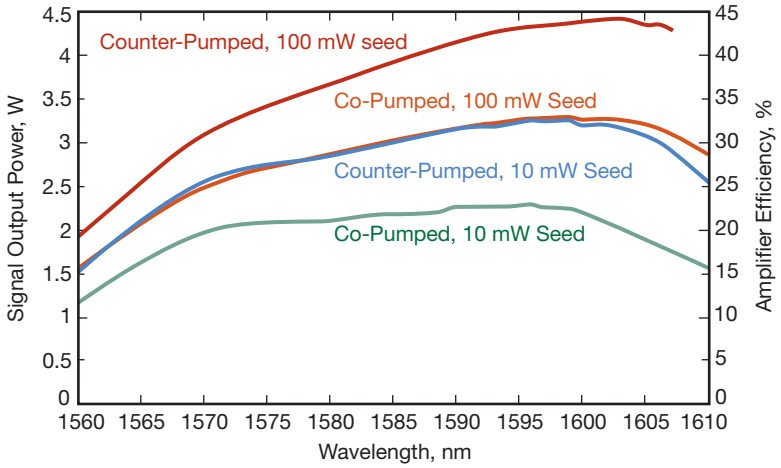

Figure 12. Optimized signal output power as a function of wavelength for various 1530-nm pumping (10 W) and seeding configurations.

ments in Section IV was not included in the calculations. There is some sensitivity, though, to varying parameters, so it is important to understand the impact of reasonable parameter changes used to obtain agreement between the modeling and experiments.

A significant unknown in the modeling is the effect of ion clustering. Our model shows that there was a negligible variation in the output powers when the clustering was varied ±0.5 percent from the nominal value of 3.6 percent quoted by Liekki. The other important aspect of high-density doping is that of concentration quenching. This usually manifests at high doping levels as a reduction of the metastable state lifetime, and is usually determined by direct measurement [18,19]. Figure 13 shows the optimization curves for nominal conditions and when the metastable state lifetime is halved due to concentration quenching. Although the reduced lifetime leads to a predicted loss of efficiency, the simulations predict that an efficiency of 40 percent can still be reached.

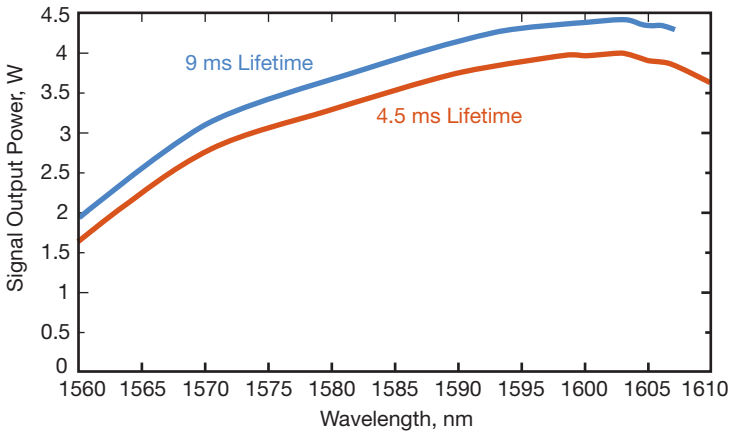

Figure 13. Optimized signal output power as a function of wavelength for 9 ms and 4.5 ms metastable state lifetime for 1530-nm counter-pumping (10 W) and 100-mW seed.

V. Conclusion

In order to improve the efficiency of fiber laser transmitters used for optical communications, resonant pumping of the Er-doped amplifier was proposed. A preliminary fiber model allowed the design of an experimental demonstration with existing commercially available components and the potential for an overall amplifier efficiency of >20 percent. The agreement between this model and the experiment was limited due to the absence of certain physical effects. Although not optimized in its performance due to the limitations of pump diodes in terms of power efficiency and broadened linewidth, the experimental results were, however, confirmed by a more detailed fiber model that pointed to an optimized design with at least >40 percent optical-to-optical efficiency in the amplifier configuration. That design is currently being implemented in a second-generation amplifier configuration using narrow-linewidth pump diodes to optimize the absorption, improved seed powers, and Er-doped fiber optimized for 1530-nm pumping, and will be reported separately with the goal of demonstrating a laser transmitter capable of >20 percent overall wall-plug optical efficiency. Future work will also address the ability to optimize the core/clad ratio of the amplifier fiber to achieve these higher efficiencies, which requires a 70 percent optical-to-optical conversion efficiency.

Acknowledgments

The technical assistance of Carlos Esproles in the experiment is gratefully acknowledged.

References

[1] N. W. Spellmeyer, D. O. Caplan, B. S. Robinson, D. Sandberg, M. L. Stevens, M. M. Willis, D. V. Gapontsev, N. S. Platonov, and A. Yusim, "A High-Efficiency Ytterbium-Doped Fiber Amplifier Designed for Interplanetary Laser Communications," Optical Fiber Communication Conference, paper OMF2, Anaheim, California, March 25–29, 2007.

[2] N. W. Spellmeyer, D. O. Caplan, and M. L. Stevens, "Design for a 5-Watt PPM Transmitter for the Mars Laser Communications Demonstration," IEEE Lasers and Electro-Optics Society (LEOS) Topical Meeting, paper TuA4.1, San Diego, California, July 25–27, 2005.

[3] P. Crump, W. Dong, M. Grimshaw, J. Wang, S. Patterson, D. Wise, M. DeFranza, S. Elim, S. Zhang, M. Bougher, J. Patterson, S. Das, J. Bell, J. Farmer, M. DeVito, and R. Martinsen, "100-W+ Diode Laser Bars Show >71% Power Conversion from 790-nm to 1000-nm and Have Clear Route to >85%," *Proceedings of SPIE*, vol. 6456, 64560M, San Jose, California, January 22, 2007.

[4] M. W. Wright, D. Zhu, and W. Farr, "Characterization of a High-Power Fiber Master Oscillator Power Amplifier (MOPA) Laser as an Optical Communications Transmitter," *The Interplanetary Network Progress Report*, vol. 42-161, Jet Propulsion Laboratory, Pasadena, California, pp. 1–12, May 15, 2005.
http://ipnpr.jpl.nasa.gov/progress_report/42-161/161F.pdf

[5] J. R. Simpson, *Rare-Earth-Doped Fiber Lasers and Amplifiers*, M.J.F. Digonnet, editor, New York: Marcel Dekker, 1993.

[6] P. Leisher, W. Dong, X. Guan, M. Grimshaw, J. Patterson, and S. Patterson, "Advancements in Broad-Area InP-Based Diode Lasers Operating from 1400-nm to >2100-nm," nLIGHT Technical Report, www.nlight.net, January 2010.

[7] M. Dubinskii, V. Ter-Mikirtychev, J. Zhanga and I. Kudryashov, "Yb-free, SLM EDFA: Comparison of 980-, 1470- and 1530-nm Excitation for the Core- and Clad-Pumping," *Proceedings of SPIE*, vol. 6952, 695205, Orlando, Florida, March 17, 2008.

[8] M. Dubinskii, J. Zhang and V. Ter-Mikirtychev, "Record-Efficient, Resonantly-Pumped, Er-Eoped Single Mode Fibre Amplifier," *Electronics Letters*, vol. 45, no. 8, pp. 400–401, April 9, 2009.

[9] D. Y. Shen, J. K. Sahu, and W. A. Clarkson, "Highly Efficient Er,Yb-Doped Fiber Laser with 188 W Free-Running and >100 W Tunable Output Power," *Optics Express*, vol. 13, no. 13, pp. 4916–4921, June 25, 2005.

[10] M. Dubinskii, J. Zhang, and V. Ter-Mikirtychev, "Highly Scalable, Resonantly Cladding-Pumped, Er-Doped Fiber Laser with Record Efficiency," *Optics Letters*, vol. 34, no. 10, pp. 1507–1509, May 15, 2009.

[11] H. M. Pask, R. J. Carman, D. C. Hanna, A. C. Tropper, C. J. Mackechnie, P. R. Barber, and J. M. Dawes, "Ytterbium-Doped Silica Fiber Lasers: Versatile Sources for the 1–1.2 μm Region," *IEEE Journal of Selected Topics in Quantum Electronics*, vol. 1, no. 1, pp. 2–13, April 1995.

[12] Mark Dubinskii, Jun Zhang, and Igor Kudryashov, "Single-Frequency, Yb-Free, Resonantly Cladding-Pumped Large Mode Area Er Fiber Amplifier for Power Scaling," *Applied Physics Letters*, vol. 93, no. 3, 031111, July 25, 2008.

[13] V. Kuhn, D. Kracht, J. Neumann, and P. Weßels, "67 W of Output Power From an Yb-Free Er-Doped Fiber Amplifier Cladding Pumped at 976 nm," *IEEE Photonics Technology Letters*, vol. 23, no. 7, pp. 432–434, April 1, 2011.

[14] J. Zhang, V. Fromzel, and M. Dubinskii, "Resonantly Cladding-Pumped Yb-Free Er-Doped LMA Fiber Laser with Record High Power and Efficiency," *Optics Express*, vol. 19, no. 6, pp. 5574–5578, March 14, 2011.

[15] M. A. Rebolledo, S. Jarabo, M. Hotoleanu, M. Karasek, E. Grolmus, and E. Jaunart, "Analysis of a Technique to Determine Absolute Values of the Stimulated Emission Cross Section in Erbium-Doped Silica Fibres from Gain Measurements," *Pure and Applied Optics*, vol. 6, no. 3, pp. 425–433, May 1997.

[16] J. R. Marciante and J. D. Zuegel, "High-Gain, Polarization-Preserving, Yb-Doped Fiber Amplifier for Low-Duty-Cycle Pulse Amplification," *Applied Optics*, vol. 45, no. 26, pp. 6798–6804, September 10, 2006.

[17] P. C. Becker, N. A. Olsson, and J. R. Simpson, *Erbium-Doped Fiber Amplifiers: Fundamentals and Technology*, San Diego, California: Academic Press, 1999, p. 193.

[18] W. Guan and J. R. Marciante, "Pump-Induced, Dual-Frequency Switching in a Short-Cavity, Ytterbium-Doped Fiber Laser," *Optics Express*, vol. 15, no. 23, pp. 14979–14992, November 12, 2007.

[19] T. Yamashita and Y. Ohishi, "Concentration and Temperature Effects on the Spectroscopic Properties of Tb^{3+} Doped Borosilicate Glasses," *Journal of Applied Physics*, vol. 102, no. 2, 123107, December 15, 2007.